$$K1K2{\cdot}K1E2 \rightleftharpoons K1K2 + K1E2 \quad (16)$$

$$K1E2{\cdot}E1E2 \rightleftharpoons K1E2 + E1E2 \quad (17)$$

$$K1K2{\cdot}E1K2 \rightleftharpoons K1K2 + E1K2 \quad (18)$$

$$E1K2{\cdot}E1K2 \rightleftharpoons 2E1K2 \quad (19)$$

Equations (1), (4)–(6), (14); equations (1), (2), (7)–(10), (15)–(17); and equations (1), (3), (11)–(13), (18), (19) were analysed simultaneously. Results are summarized in Table 2.

Received 8 September 1997; accepted 1 September 1998.

1. von Kiedrowski, G. A self-replicating hexadeoxynucleotide. *Angew. Chem. Int. Edn Engl.* **25,** 932–935 (1986).
2. von Kiedrowski, G., Wlotzka, B. & Helbing, J. Sequence dependence of template-directed syntheses of hexadeoxynucleotide derivatives with 3′-5′ pyrosphosphate linkage. *Angew. Chem. Int. Edn Engl.* **28,** 1235–1237 (1989).
3. von Kiedrowski, G., Wlotzka, B., Helbing, J., Matzen, M. & Jordan, S. Parabolic growth of a self-replicating hexadeoxynucleotide bearing a 3′-5′ phosphoamidate linkage. *Angew. Chem. Int. Edn Engl.* **30,** 423–426 (1991).
4. Sievers, D. & von Kiedrowski, G. Self-replication of complementary nucleotide-based oligomers. *Nature* **369,** 221–224 (1994).
5. Achilles, T. & von Kiedrowski, G. A self-replicating system from *three* starting materials. *Angew. Chem. Int. Edn Engl.* **32,** 1198–1201 (1993).
6. Zielinski, W. S. & Orgel, L. E. Autocatalytic synthesis of a tetranucleotide analogue. *Nature* **327,** 346–347 (1987).
7. Li, T. & Nicolaou, K. C. Chemical self-replication of palindromic duplex DNA. *Nature* **369,** 218–221 (1994).
8. Lee, D. H., Granja, J. R., Martinez, J. A., Severin, K. & Ghadiri, M. R. A self-replicating peptide. *Nature* **382,** 525–528 (1996).
9. Severin, K., Lee, D. H., Kennan, A. J. & Ghadiri, M. R. A synthetic peptide ligase. *Nature* **389,** 706–709 (1997).
10. Lee, D. H., Granja, J. A., Severin, K., Yokobayashi, Y. & Ghadiri, M. R. Emergence of symbiosis in peptide self-replication through a hypercyclic network. *Nature* **390,** 591–594 (1997).
11. Yao, S., Ghosh, I., Zutshi, R. & Chmielewski, J. A pH-modulated, self-replicating peptide. *J. Am. Chem. Soc.* **119,** 10559–10560 (1997).
12. Yao, S., Ghosh, I., Zutshi, R. & Chmielewski, J. A self-replicating peptide under ionic control. *Angew. Chem. Int. Edn Engl.* **37,** 478–481 (1998).
13. Tjivikua, T., Ballester, P. & Rebek, J. Jr A self-replicating system. *J. Am. Chem. Soc.* **112,** 1249–1250 (1990).
14. Nowick, J. S., Feng, Q., Tjivikua, T., Ballester, P. & Rebek, J. Jr Kinetic studies and modeling of a self-replicating system. *J. Am. Chem. Soc.* **113,** 8831–8839 (1991).
15. Wintner, E. A., Conn, M. M. & Rebek, J. Jr Self-replicating molecules: a second generation. *J. Am. Chem. Soc.* **116,** 8877–8884 (1994).
16. Wintner, E. A., Tsao, B. & Rebek, J. Jr Evidence against an alternative mechanism for a self-replicating system. *J. Org. Chem.* **60,** 7997–8001 (1995).
17. Orgel, L. E. Unnatural selection in chemical systems. *Acc. Chem. Res.* **28,** 109–118 (1995).
18. Zhou, N. E., Kay, C. M. & Hodges, R. S. The role of interhelical ionic interactions in controlling protein folding and stability. *De novo* designed synthetic two-stranded alpha-helical coiled-coils. *J. Mol. Biol.* **237,** 500–512 (1994).
19. Dawson, P. E., Muir, T. W., Clark-Lewis, I. & Kent, S. B. Synthesis of proteins by native chemical ligation. *Science* **266,** 776–779 (1994).
20. Kramer, F. R., Mills, D. R., Cole, P. E., Nishihana, T. & Spiegelman, S. Evolution in vitro: sequence and phenotype of a mutant RNA resistant to ethidium bromide. *J. Mol. Biol.* **89,** 719–736 (1974).

Supplementary information is available on *Nature*'s World-Wide Web site (http://www.nature.com) or as paper copy from the London editorial office of *Nature*.

Acknowledgements. This work was supported by the NSF.

Correspondence and requests for materials should be addressed to J.C. (e-mail: chml@cv1.chem.purdue.edu).

A new model for Proterozoic ocean chemistry

D. E. Canfield

Biological Institute, Odense University, Campusvej 55, 5230 Odense M, Denmark

There was a significant oxidation of the Earth's surface around 2 billion years ago (2 Gyr)[1–4]. Direct evidence for this oxidation comes, mostly, from geological records of the redox-sensitive elements Fe and U reflecting the conditions prevailing during weathering[1–3]. The oxidation event was probably driven by an increased input of oxygen to the atmosphere arising from an increased sedimentary burial of organic matter between 2.3 and 2.0 Gyr[5]. This episode was postdated by the final large precipitation of banded iron formations around 1.8 Gyr[1,2]. It is generally believed that banded iron formations precipitated from an ocean whose bottom waters contained significant concentrations of dissolved ferrous iron, and that this sedimentation process terminated when aerobic bottom waters developed, oxidizing the iron and thus removing it from solution[1,2]. In contrast, I argue here that anoxic bottom waters probably persisted until well after the deposition of banded iron formations ceased; I also propose that sulphide, rather than oxygen, was responsible for removing iron from deep ocean water. The sulphur-isotope record supports this hypothesis as it indicates increasing concentrations of oceanic sulphate, starting around 2.3 Gyr[6], leading to increasing rates of sulphide production by sulphate reduction. The increase in sulphide production became sufficient, around 1.8 Gyr, to precipitate the total flux of iron into the oceans. I suggest that aerobic deep-ocean waters did not develop until the Neoproterozoic era (1.0 to ~0.54 Gyr), in association with a second large oxidation of the Earth's surface. This new model is consistent with the emerging view of Precambrian sulphur geochemistry and the chemical events leading to the evolution of animals, and it is fully testable by detailed geochemical analyses of preserved deep-water marine sediments.

The oxygen content of deep ocean waters is controlled mainly by the balance between the supply of oxygen from downwelling surface waters and oxygen consumption by decomposing organic debris[7]. The oxidation of submarine hydrothermal inputs, by comparison, requires 2 to 3 orders of magnitude less oxygen than the oxidization of organic matter[8]. In the modern ocean, the downwelling of cold high-latitude surface waters saturated with oxygen results in largely aerobic bottom waters[7]. Furthermore, primary production, fuelled by nutrients dissolved in upwelling deep ocean water, produces insufficient organic matter to exhaust the oxygen in deep waters as the organic matter sinks and decomposes[7]. Deep-water anoxia could occur, however, by a reduction in the concentration of oxygen in downwelling surface waters, an increase in the nutrient concentration of the oceans (allowing more primary production, and consequently a greater organic carbon rain to the deep ocean, at equivalent rates of ocean ventilation), or by an increase in the efficiency of nutrient utilization, which is particularly poor in the modern high-latitude ocean[7].

A simple three-box model, used primarily with respect to the ice-age ocean, has been useful in exploring the regulation of the oxygen content of deep ocean waters[7]. The ocean is divided into a deep ocean box (d), and two surface boxes: one representing the region of bottom water formation (f) and the other the remainder of the surface ocean (s). In simplified form, the concentration of oxygen in the deep ocean is given by[7]:

$$O_2(d) = O_2(f) - r[P(d) - P(f)] \quad (1)$$

where O_2 is oxygen concentration (micromolar, μM), P is phosphate concentration (μM), with phosphate taken as the limiting nutrient in primary production, and r is the Redfield ratio between O_2 consumption and phosphate production during organic matter mineralization, taken here as 169 (ref. 7). Estimates for r vary between 120 and 200 (ref. 9); in this range, however, the value of this parameter does not alter my major conclusions. The difference $[P(d) - P(f)]$ represents the amount of phosphorus in upwelling deep water that is used during primary production.

The model can be used to explore how the oxygen content of deep ocean waters ($O_2(d)$) responds to variable levels of both surface water oxygen (represented by $O_2(f)$) and nutrient availability $[P(d) - P(f)]$ (Fig. 1). A drop in $O_2(f)$, for example, means that a smaller value of $[P(d) - P(f)]$ is required to maintain aerobic conditions in the deep ocean. In physical terms, lower nutrient availability reduces primary production, and therefore lowers oxygen demand in the deep ocean by decomposing sunken organic matter. This is why lower nutrient availability allows aerobic conditions to persist as values of $O_2(f)$ drop. When $O_2(f)$ falls to 25 μM, aerobic conditions are nearly impossible to maintain when there is any appreciable phosphorus in the oceans. With the present-

day [P(d) − P(f)] value of 0.91 μM (ref. 7), concentrations of O_2(f) exceeding 150–200 μM are required to maintain even minimally aerobic deep ocean conditions. The concentration of O_2(f) in the modern ocean is ~325 μM (ref. 7), which is in approximate equilibrium with the atmosphere. Water-column primary production and air injection can drive O_2(f) to higher than equilibrium levels, although oversaturation rarely exceeds 10–20 μM O_2 (ref. 10), and may be much less.

This analysis shows that the development of aerobic deep ocean waters requires a combination of either low atmospheric oxygen levels and extremely low nutrient availability, or high atmospheric oxygen levels and nutrient availability comparable to the present-day ocean. The exogenic inventory of phosphorus has probably not varied greatly over much of geological time, meaning that levels of nutrient availability have also not varied greatly[2]. Therefore, Proterozoic (2.5–0.54 Gyr) oceans probably had phosphorus levels similar to the modern ocean. Under these circumstances, aerobic deep ocean water would have required high levels of atmospheric oxygen—within a factor of 2 or 3 of the present level (Fig. 1).

Several lines of evidence, however, suggest that atmospheric oxygen did not reach these high levels until the Neoproterozoic era, considerably later than the last period of major banded iron formation (BIF) deposition. The evidence includes the late Proterozoic rise of animals[1,11] and colourless sulphur bacteria[12], and the large increase in stable sulphur isotope fractionation at 0.6–1.0 Gyr[12]. All of these have been linked to oxygen levels rising to >10–20% of present-day levels[1,11–13], and are roughly coincident with a second major input pulse of oxygen to the atmosphere[14].

Here I propose an alternative model for the development of ocean chemistry during the Precambrian aeon, which is consistent with a two-stage rise in atmospheric oxygen levels[1,2,4,11]. The first stage, at ~2.3–2.0 Gyr, produced enough oxygen to influence the chemical behaviour of many redox-sensitive elements during weathering, but not enough to create an aerobic deep ocean. During this period, seawater sulphate levels increased, stimulating sulphate reduction and generating enough sulphide to remove dissolved ferrous iron as iron sulphides. The second stage, in the Neoproterozoic era, generated enough oxygen to sweep the deep ocean of sulphide, and resulted in the many biological and geochemical innovations that occurred at this time.

A transition from an Fe-rich to a sulphidic early Proterozoic ocean is consistent with the isotope record of non-hydrothermal sedimentary sulphides (Fig. 2; see also ref. 6). A prominent feature of this record is a large increase in the isotope difference between seawater sulphate and sulphide at ~2.20–2.30 Gyr[6,15]. The small fractionations before 2.20–2.30 Gyr are generally comparable to the small (≤4‰) fractionations reported for bacterial sulphate reduction with ≤ 1 mM sulphate[16]. Therefore, 1 mM may be a reasonable upper limit for the concentration of seawater sulphate before 2.20–2.30 Gyr[6,15] (for a different view, see ref. 17). The increase in fractionation at 2.20–2.30 Gyr is thus consistent with a rise in seawater sulphate concentration to >1 mM, where much larger fractionations (4–46 ‰) by sulphate-reducing bacteria are expressed[5,15,18]. An increase in sulphate concentration at 2.20–2.30 Gyr would also coincide approximately with the timing of the first stage of Earth surface oxidation[3]. It is possible that in some restricted ocean basins before 2.2–2.3 Gyr—where, for example, mineral sulphate deposition occurred, or anoxygenic photosynthesis was particularly active—there might have been elevated concentrations of sulphate[15]. Under these circumstances, we might expect there to have been enhanced isotope fractionation during sulphate reduction, although the isotope record provides few, if any, compelling examples (Fig. 2).

Models and empirical observations of sedimentary sulphur contents both show that low concentrations of sulphate, for example the

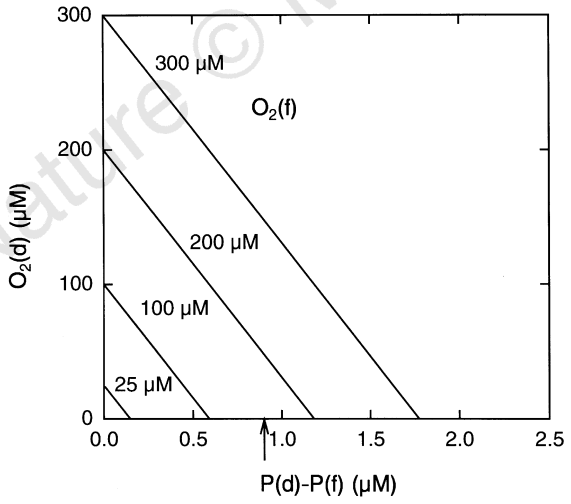

Figure 1 The relationship between deep-water oxygen concentration (O_2(d)) and phosphorus availability (represented by [P(d) − P(f)]) in the oceans. Solid lines show constant surface-water oxygen levels (O_2(f)). The model results have been calculated from equation (1), assuming a three-box ocean and well-mixed boxes[7]. The figure shows, for example, that with 300 μM O_2(f), deep-water anoxia occurs when phosphorus availability rises to ~1.6 μM. With no nutrients in the ocean, bottom water oxygen remains the same as surface values. Present-day phosphorus availability is ~0.9 μM (arrow); this requires O_2(f) values of ⩾160–170 μM to maintain oxygen in deep-ocean waters. The three-box model is a highly simplified picture of ocean dynamics which only gives broad averages. The absence of information on Precambrian ocean circulation, however, justifies this simplified approach to understanding the relationship between atmospheric oxygen levels and Precambrian ocean anoxia. See text for details.

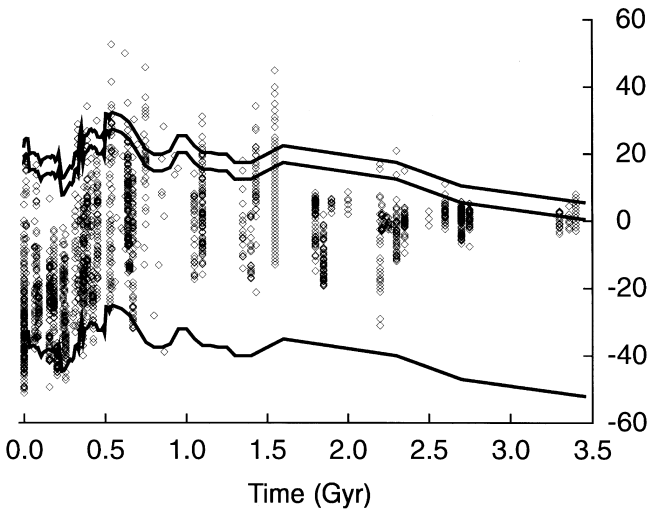

Figure 2 The isotope composition of sedimentary sulphides of probable biological origin over geological time. This excludes sulphides of obviously hydrothermal origin, those hosted in non-sedimentary rocks, and those from sediments that have experienced beyond greenschist phase metamorphism. Shown for comparison is the isotope composition of seawater sulphate, mostly obtained from measuring the isotope composition of evaporitic anhydrite or gypsum. Before 2.2 Gyr the isotope composition of sulphate is determined mostly from barites. The two upper lines show the isotope composition of sulphate. The range (5‰) represented by the pair of lines shows the uncertainty in the inferred isotopic composition of seawater sulphate. However, before 1 Gyr, knowledge of the isotope composition of seawater sulphate is constrained by a lack of data, resulting in a loss of detail. The lower line shows the isotope composition of sulphate displaced by 55‰ to more ^{34}S-depleted values. Comparison of the isotope composition of sulphides and this lower line demonstrates how the fractionation between sulphate and sedimentary sulphides has increased over time. Data are taken partly from an earlier compilation[12]; additional data sources are available as Supplementary Information.

50–500 μM typically found in freshwater lakes, limits the rate of sulphate reduction[19,20]. An increase in the sulphate concentration of low sulphate systems will therefore result in increased rates of sulphate reduction. Once the rate of sulphate reduction exceeded the rate at which sulphide-reactive Fe was delivered to early Proterozoic oceans, dissolved Fe would have been completely removed from the oceans. It is possible that sulphate concentrations rose gradually between 2.3 Gyr, when high rates of carbon burial first commenced[4], and 1.8 Gyr, when the last of the major BIFs were deposited[2]. This would mean that levels of sulphate first exceeded those required to produce large isotope fractionations at 2.2–2.3 Gyr, whereas sulphate reduction rates first exceeded rates of Fe delivery to the oceans at ~1.8 Gyr.

In the Neoproterozoic era, there was a return to a much smaller-scale deposition of BIFs[21], for example those found in the Rapitan Group (~0.70–0.75 Gyr) of the Mackenzie Mountains, Canada. These BIFs are intimately associated with glacial deposits, and they were probably deposited during periods of ocean stagnation promoted by glaciation[21]. It is not known whether the dissolved Fe that precipitated as BIFs accumulated throughout the ocean basin, or whether it was only present in regions analogous to modern-day oxygen minimum zones. In either case, the accumulation of dissolved Fe rather than sulphide shows that there were low rates of sulphate reduction, compared to rates of Fe delivery, within broad anoxic regions of the ocean. A possible explanation is a reduction of sulphate concentration during ocean stagnation, to levels inhibiting sulphate reduction, similar to the conditions found in the early Proterozoic. A low water-column concentration of sulphate during the Neoproterozoic era has previously been advocated[22] to explain the preponderance of ^{34}S-enriched sedimentary sulphides found from this time. It is possible that the concentration of seawater sulphate did not rise to near present levels until after the second stage of Earth-surface oxidation in the Late Neoproterozoic era.

In the modern oceans, there is enough sulphide produced by sulphate reduction to precipitate about seven times the delivery flux of iron to the oceans (Table 1). This does not occur, and oxidized iron persists in many modern marine sediments, because there is intense sulphide oxidation (by oxygen or other oxidized compounds) in sediments[12]. However, with modern-day fluxes of reactive Fe and rates of sulphate reduction, dramatically reduced atmospheric oxygen would promote ocean anoxia and the development of sulphidic ocean conditions. Similar conditions of excess sulphide production with respect to Fe delivery are envisaged for middle to late Proterozoic oceans. Late Proterozoic glacial intervals are an exception, where ocean stagnation is proposed to have drawn down sulphate levels so that rates of sulphate reduction were less than those of Fe delivery, leading to renewed BIF deposition.

Table 1 Comparison of delivery flux of reactive iron and sulphate reduction rate in the modern ocean

Reactive Fe from terrigenous sources	4.9×10^{12} mol yr^{-1}
Hydrothermal Fe input	1.7×10^{11} mol yr^{-1}
Total reactive Fe delivery flux	5.1×10^{12} mol yr^{-1}
Maximum sulphide removal as FeS_2	10.2×10^{12} mol yr^{-1}
Sulphate-reduction rate	73×10^{12} mol yr^{-1}

I computed the delivery flux of sulphide-reactive Fe to the oceans by combining the average concentration of total Fe in river particulates (4.4 wt%)[29], and the proportion of this total Fe that is sulphide-reactive (0.27; ref. 25), with the flux of terrigenous particulates to ocean. The composition of river particulates is assumed to represent terrigenous material in general. The total flux of terrigenous particulates (23×10^{15} g yr^{-1}) consists of a river-derived component[30] of 20×10^{15} g yr^{-1} and 1.5×10^{15} g yr^{-1} each from glacial discharge and wind-blown dust. The terrigenous particle flux is added the input from mid-ocean ridge hydrothermal vents, computed by combining the average concentration of Fe in vent fluids with the fluid flow through the high-temperature vents[8]. The potential maximum removal rate of sulphide (as pyrite, FeS_2) is equivalent to twice the delivery flux of Fe to the oceans. Global rates of sulphate reduction are calculated here from a literature compilation of 220 sulphate-reduction rate determinations. Rates were organized into eight different sedimentary environments, including shallow intertidal, coastal upwelling, estuaries and bays, high deposition shelf, low deposition shelf, slope, rise and abyss. Rates were averaged and then multiplied by the ocean area for each environment to yield total rates of sulphate reduction.

I believe that there should be direct evidence for a middle- to late-Proterozoic sulphide-rich ocean in the geochemical record of preserved deep-water marine sediments. Unfortunately, there are very few geochemical reports from this time that can be used to explore for euxinic conditions. A non-clastic source of Fe has been identified in the deep-water black shales of the Newland Formation of the Mesoproterozoic (1.35–1.4 Gyr) Belt Supergroup in the United States[23]. A similar non-clastic Fe source has been identified in the laminated euxinic sediments of the Black Sea[24], and this non-clastic Fe, associated with sulphide, requires a euxinic basin for its deposition[24,25]. Thus, the shales of the Newland Formation could have been deposited under euxinic conditions, but further analysis is required to substantiate this conclusion. Euxinic conditions have also been proposed during the deposition of the Mesoproterozoic Nonesuch Shale (1.1 Gyr) in the United States[26], for some intervals of the Velkerri Formation (1.45 Gyr), McArthur Basin, Australia[27], and for black shales from the Upper Proterozoic Hedmark Group, Norway[28].

These few reports should not, however, be taken as proof of a sulphide-rich ocean in the middle to late Proterozoic; my study should be considered as a basis for investigating middle Proterozoic sediment geochemistry, with a view to understanding depositional conditions. However, the development of a middle-Proterozoic sulphidic ocean, as proposed here, best explains the available geochemical and biological information on the course of Earth-surface change during the Proterozoic aeon. □

Received 23 October 1997; accepted 17 September 1998.

1. Cloud, P. E. Jr A working model of the primitive Earth. *Am. J. Sci.* **272,** 537–548 (1972).
2. Holland, H. D. *The Chemical Evolution of the Atmosphere and Oceans* (Princeton Univ. Press, Princeton, 1984).
3. Holland, H. D. & Beukes, N. A paleoweathering profile from Griqualand West, South Africa: evidence for a dramatic rise in atmospheric oxygen between 2.2 and 1.9 bybp. *Am. J. Sci.* **290-A,** 1–34 (1990).
4. Des Marais, D. J., Strauss, H. Summons, R. E. & Hayes, J. M. Carbon isotope evidence for the stepwise oxidation of the Proterozoic environment. *Nature* **359,** 605–609 (1992).
5. Karhu, J. A. & Holland, H. D. Carbon isotopes and the rise of atmospheric oxygen. *Geology* **24,** 867–870 (1996).
6. Hayes, J. M., Lambert, I. B. & Strauss, H. in *The Proterozoic Biosphere: A Multidisciplinary Study* (eds Schoff, J. W. & Klein, C.) 129–134 (Cambridge Univ. Press, 1992).
7. Sarmiento, J. L., Herbert, T. D. & Toggweiler, J. R. Causes of anoxia in the world ocean. *Glob. Biogeochem. Cycles* **2,** 115–128 (1988).
8. Ridge/vents Workshop Group. In *Global Impact of Submarine Hydrothermal Processes* (eds Kadko, D., Baker, E., Alt, J. & Baross, J.) 4–15 (NSF RIDGE Initiative and NOAA Vents Program, 1994).
9. Shaffer, G. Biogeochemical cycling in the global ocean 2. New production, Redfield ratios, and remineralization in the organic pump. *J. Geophys. Res.* **101,** 3723–3745 (1996).
10. Emerson, S., Quay, P. D., Stump, C. & Schudlich, R. Chemical tracers of productivity and respiration in the subtropical Pacific Ocean. *J. Geophys. Res.* **100,** 15873–15887 (1995).
11. Knoll, A. H. in *Origin and Early Evolution of the Metazoa* (eds Lipps, J. H. & Signor, P. W.) 53–84 (Plenum, New York, 1992).
12. Canfield, D. E. & Teske, A. Late proterozoic rise in atmospheric oxygen concentration inferred from phylogenetic and sulphur-isotope studies. *Nature* **382,** 127–132 (1996).
13. Berkner, L. V. & Marshall, L. C. On the origin and rise of oxygen concentration in the Earth's atmosphere. *J. Atmos. Res.* **22,** 225–261 (1965).
14. Knoll, A. H., Hayes, J. M., Kaufman, A. J., Swett, K. & Lambert, I. B. Secular variation in carbon isotope ratios from Upper Proterozoic successions of Svalbard and East Greenland. *Nature* **321,** 832–838 (1986).
15. Cameron, E. M. Sulphate and sulphate reduction in early Precambrian oceans. *Nature* **296,** 145–148 (1982).
16. Harrison, A. G. & Thode, H. G. Mechanisms of the bacterial reduction of sulfate from isotope fractionation studies. *Trans. Faraday Soc.* **53,** 84–92 (1958).
17. Ohmoto, H., Kakegawa, T. & Lowe, D. R. 3.4-billion-year-old biogenic pyrites from Barberton, South Africa: Sulfur isotope evidence. *Science* **262,** 555–557 (1993).
18. Habicht, K. S. & Canfield, D. E. Sulphur isotope fractionation in modern microbial mats and the evolution of the sulphur cycle. *Nature* **382,** 342–343 (1996).
19. van Cappellen, P. & Wang, Y. in *Metal Contaminated Sediments* (ed. Allen, H. E.) 21–64 (Ann Arbor, Chelsea, Michigan, 1995).
20. Berner, R. A. & Raiswell, R. Burial or organic carbon and pyrite sulfur in sediments over geologic time. *Geochim. Cosmochim. Acta* **47,** 855–862 (1983).
21. Beukes, N. J. & Klein, C. in *The Proterozoic Biosphere: A Multidisciplinary Study* (eds Schoff, J. W. & Klein, C.) 147–151 (Cambridge Univ. Press, 1992).
22. Logan, G. A., Hayes, J. M., Hieshima, G. B. & Summons, R. E. Terminal Proterozoic re-organization of biogeochemical cycles. *Nature* **376,** 53–56 (1995).
23. Schieber, J. Anomalous iron distribution in shales as a manifestation of "non-clastic iron" supply to sedimentary basins: relevance for pyritic shales, base-metal mineralization, and oolitic ironstone deposits. *Mineral. Deposita* **30,** 294–302 (1995).
24. Canfield, D. E., Lyons, T. W. & Raiswell, R. A model for iron deposition to euxinic Black Sea sediments. *Am. J. Sci.* **296,** 818–834 (1996).
25. Raiswell, R. & Canfield, D. E. Sources of iron for pyrite formation in marine sediments. *Am. J. Sci.* **298,** 219–245 (1998).
26. Imbus, S. W., Macko, S., Elmore, R. D. & Engel, M. Stable isotope (C,S,N) and molecular studies on the Precambrian Nonesuch Shale (Wisconsin–Michigan, USA): evidence for differential preservation rates, depositional environment and hydrothermal influence. *Chem. Geol.* **101,** 255–281 (1992).
27. Jackson, M. J. & Raiswell, R. Sedimentology and carbon–sulphur geochemistry of the Velkerri Formation, a mid-Proterozoic potential oil source in northern Australia. *Precambr. Res.* **54,** 81–108 (1991).

28. Vidal, G. & Nystuen, J. P. Micropaleontology, depositional environment, and biostratigraphy of the Upper Proterozoic Hedmark Group, Southern Norway. *Am. J. Sci.* **290-A,** 170–211 (1990).
29. Canfield, D. E. The geochemistry of river particulates from the continental United States: major elements. *Geochim. Cosmochim. Acta* **61,** 3349–3365 (1997).
30. Milliman, J. D. & Syvitski, J. P. M. Geomorphic/tectonic control of sediment discharge to the ocean: the importance of mountainous rivers. *J. Geol.* **100,** 525–544 (1992).

Supplementary information is available on *Nature*'s World-Web site (http://www.nature.com) or as paper copy from the London editorial office of *Nature*.

Acknowledgements. I thank J. Hayes, B. Thamdrup, D. Des Marais and A. Knoll for comments on the manuscript. Financial support came from the Danish National Science Research Council (SNF) and the Danish National Research Foundation (Danmarks Grundforskningsfond). This Letter is dedicated to the memory of H. Jannasch.

Correspondence and requests for materials should be addressed to D.E.C. (e-mail: dec@biology.ou.dk).

Low-latitude glaciation and rapid changes in the Earth's obliquity explained by obliquity–oblateness feedback

Darren M. Williams*, James F. Kasting† & Lawrence A. Frakes‡

** School of Science, Penn State Erie, The Behrend College, Station Road, Erie, Pennsylvania 16563-0203, USA*
† Department of Geosciences, The Pennsylvania State University, 443 Deike Building, University Park, Pennsylvania 16802, USA
‡ Department of Geology and Geophysics, University of Adelaide, Adelaide, South Australia 5005, Australia

Palaeomagnetic data suggest that the Earth was glaciated at low latitudes during the Palaeoproterozoic[1,2] (about 2.4–2.2 Gyr ago) and Neoproterozoic[3–8] (about 820–550 Myr ago) eras, although some of the Neoproterozoic data are disputed[9,10]. If the Earth's magnetic field was aligned more or less with its spin axis, as it is today, then either the polar ice caps must have extended well down into the tropics—the 'snowball Earth' hypothesis[8]—or the present zonation of climate with respect to latitude must have been reversed. Williams[11] has suggested that the Earth's obliquity may have been greater than 54° during most of its history, which would have made the Equator the coldest part of the planet[12]. But this would require a mechanism to bring the obliquity down to its present value of 23.5°. Here we propose that obliquity–oblateness feedback[13] could have reduced the Earth's obliquity by tens of degrees in less than 100 Myr if the continents were situated so as to promote the formation of large polar ice sheets. A high obliquity for the early Earth may also provide a natural explanation for the present inclination of the lunar orbit with respect to the ecliptic (5°), which is otherwise difficult to explain.

The most straightforward explanation for low-latitude glaciation is simply that the climate was very cold in Precambrian times as a consequence of reduced solar luminosity[14], uncompensated by high levels of greenhouse gases. It is difficult to explain, however, how the ice caps could have extended to low latitudes without causing the extinction of most or all surface life. Energy-balance climate models[14,15] suggest that runaway glaciation should occur if the ice line extends equatorwards of 25–30° latitude. At least some of the ancient glaciations appear to have occurred at latitudes much lower than this[8]. Had the ice line moved down below the critical latitude for stability, the Earth should have switched into a globally glaciated state in which even the oceans would have frozen down to a depth of ~1 km, provided that the thickness was limited by the efficiency of heat flow through the ice. If this had occurred during the Neoproterozoic era, the Earth could eventually have escaped from this state by atmospheric build-up of volcanically released CO_2, which would have warmed the surface and melted the ice[15]. However, this process would have required $\sim 10^6$–10^7 years, during which time the ocean and all marine organisms would have been deprived of sunlight. This is in apparent conflict with evidence for the continuous presence of photosynthetic marine organisms in the geological record, although some authors[8] believe that this is exactly what happened.

The high-obliquity hypothesis[11] of Williams can resolve this climate paradox because high latitudes could have remained ice-free while the tropics were glaciated. A potentially damaging counter-argument has been presented by Vanyo and Awramik[16], based on the sinusoidal growth pattern of an 850-Myr-old stromatolite which suggests a planetary obliquity of 26.5° at that time. This argument presumes that the stromatolite growth face remained perpendicular to the Sun's noontime rays throughout the course of the year. Heliotropism has indeed been seen in modern columnar stromatolites in Australia and Yellowstone[17], but in no case has it been shown that the growth pattern accurately tracks the minimum daily solar zenith angle over the year. Hence the main argument for a low obliquity during the late Proterozoic seems inconclusive.

For the high-obliquity hypothesis to be viable, one needs to identify a mechanism that could have caused the Earth's obliquity to decrease by several tens of degrees between ~600 Myr ago—the age of the youngest low-latitude glacial deposits[3–5]—and 430 Myr ago, when palaeotidal data suggest that the obliquity was close to its present value[11]. Williams himself suggested that core–mantle dis-

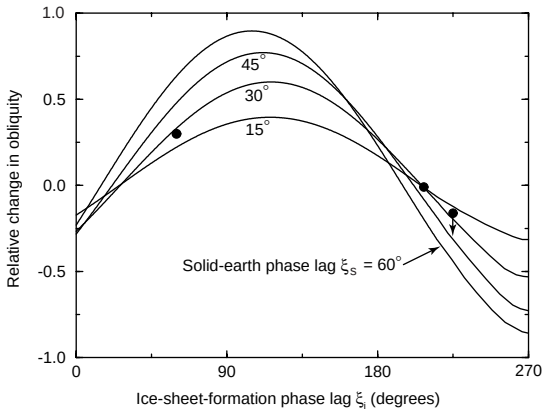

Figure 1 Relative rate of obliquity drift as a function of a ice-sheet-formation phase lag. Averaged over a precession cycle, the rate of obliquity drift may be written[13,22] $d\theta/dt = K(\Delta J_2/J_2)[\sin(\xi_i) - f(\xi_s + \xi_i)]$, where θ is the mean obliquity, and the constant K is a function of various dynamical and geophysical parameters appearing in the equations of precession[12,22]. The ellipticity coefficient J_2 is equal to $(C - A)/M_\oplus R_\oplus^2$, where C and A are Earth's principal inertial moments. The planetary oblateness is assumed to vary sinusoidally and to lag the phase of the obliquity-insolation cycle by an angle ξ_i. (In reality, ice-sheet response to insolation may be much more complicated.) The amplitude of the oblateness variation, $\Delta J_2/J_2$, represents the maximum change that could ever be realized by lowering sea level and loading Earth's continents with ice. A second oblateness variation, which opposes the first, results from isostatic adjustment of the solid Earth and is assumed to lag ice volume by ξ_s. The long response time ($\sim 10^4$ yr) of the viscous upper mantle to changes in ice volume allows the solid-Earth variation to cancel only a fraction, $f(\xi_s)\Delta J_2/J_2$, of the water-ice variation, where the fractional amplitude may be written[22] $f(\xi_s) = 0.8 - 0.8\xi_s/90°$. Shown are the rate and direction of obliquity drift for different values of the phase lags ξ_i and ξ_s. Plotted on the vertical axis is the quantity $[\sin(\xi_i) - f(\xi_s)\sin(\xi_s + \xi_i)]$. The filled circles mark the values of ξ_i used for the three calculations shown in Fig. 3. The solid-Earth phase lag ξ_s, which depends in the period of the obliquity oscillation in the Precambrian times (ref. 22), was initialized to 28° for each run. For the case when $\xi_i = 230°$, the value ξ_s grows from 28° to 45° over 100 Myr (indicated by an arrow) as a result of an increase to the ice-loading frequency as the obliquity drifts downward.